AIAA JOURNAL
Vol. 45, No. 8, August 2007

Technical Notes

TECHNICAL NOTES are short manuscripts describing new developments or important results of a preliminary nature. These Notes should not exceed 2500 words (where a figure or table counts as 200 words). Following informal review by the Editors, they may be published within a few months of the date of receipt. Style requirements are the same as for regular contributions (see inside back cover).

High-Performance Airfoil Using Coflow Jet Flow Control

Ge-Cheng Zha*
University of Miami, Coral Gables, Florida 33124
Bruce F. Carroll†
University of Florida, Gainesville, Florida 32611-6250
Craig D. Paxton‡ and Clark A. Conley§
University of Miami, Coral Gables, Florida 33124
and
Adam Wells¶
University of Florida, Gainesville, Florida 32611-6250

DOI: 10.2514/1.20926

I. Introduction

TO ACHIEVE revolutionary aircraft performance, advanced technologies should be pursued to drastically reduce the weight of aircraft and fuel consumption and significantly increase aircraft mission payload and maneuverability. Both the military and commercial aircraft will benefit from the same technology. Flow control is a promising technology to break through the limits of the conventional aerodynamic concepts.

Recently, a novel active airfoil flow control concept with zero-net mass flux, the coflow jet (CFJ) airfoil, has been developed by Zha et al. [1–5]. The CFJ airfoil achieves three effects simultaneously in a dramatic fashion: lift augmentation, stall margin increase, and drag reduction. The energy expenditure of the CFJ airfoil is low [1], and the CFJ airfoil concept is straightforward to implement. The CFJ airfoil may create a new concept of an "engineless" airplane, which uses the CFJ to generate both lift and thrust without conventional propulsion systems of propellers or jet engines [6].

A CFJ airfoil [1–5] uses an injection slot near the leading edge (LE) and a suction slot near the trailing edge (TE) on the airfoil suction surface. Similar to tangential blowing, the LE jet is in the same direction of the main flow, but the same amount of mass flow that is injected is removed via suction near the TE, resulting in zero-net mass-flux flow control. A proposed fundamental mechanism [2] is that the severe adverse pressure gradient on the suction surface strongly augments turbulent mixing between the main flow and the jet [7]. The mixing then creates the lateral transport of energy from the jet to the main flow and enables the main flow to overcome the large adverse pressure gradient and remain attached at high angle of attack (AOA). The stall margin is hence significantly increased. At the same time, the high-momentum jet drastically increases the circulation, which significantly augments lift, reduces drag, or even generates thrust (negative drag). The objective of this paper is to demonstrate the high performance of the CFJ airfoil with the wind-tunnel test results.

Presented as Paper 1260 at the AIAA 43rd Aerospace Sciences Meeting and Exhibit Conference, Reno, NV, 10–13 January 2005; received 6 November 2005; revision received 16 April 2007; accepted for publication 16 April 2007.

*Associate Professor, Department of Mechanical and Aerospace Engineering; gzha@miami.edu. Member AIAA.
†Associate Professor, Department of Mechanical and Aerospace Engineering. Associate Fellow AIAA.
‡Graduate Student, Department of Mechanical and Aerospace Engineering; Current Address: Boeing Company, Phantom Works, Huntsville, AL.
§Senior Undergraduate Student, Department of Mechanical and Aerospace Engineering.
¶Graduate Student, Department of Mechanical and Aerospace Engineering.

II. CFJ Airfoil Geometry

Figure 1 shows the baseline airfoil, NACA0025, and the CFJ airfoil, namely, CFJ0025-065-196 airfoil, which has the injection slot height of 0.65% of the chord and the suction slot height of 1.96% of the chord. The injection and suction slots are located at 7.11 and 83.18% of the chord from the leading edge. The slot faces are normal to the suction surface to make the jet tangential to the main flow. More detailed airfoil geometric data and naming convention of the CFJ airfoil are given in [3,4].

III. Results and Discussion

The chord length of the airfoil is 0.1527 m and the freestream Mach number is about 0.11. This gives the Reynolds number about 3.8×10^5, which is in the laminar/transitional region. To make the boundary layer fully turbulent so as to mimic the realistic flight conditions, the airfoil leading edge is tripped to trigger the turbulence. The detailed setup of wind-tunnel experiments and data uncertainty are given in [3,4].

A. CFJ Airfoil Performance

Figure 2 is the comparison of the measured lift coefficient for the baseline NACA0025 airfoil and the CFJ0025-065-196 airfoil with the injection total pressure coefficients given in the legend. During a test, the injection total pressure is held as constant while the AOA varies. A higher injection total pressure will yield a higher injection momentum coefficient, and hence a higher lift coefficient and stall margin. The bottom two curves with circle and cross symbols are for the baseline NACA0025 airfoil with and without LE trip. It shows that the one with trip delays stall by about 4 deg of AOA. This is because the fully turbulent boundary layer with the trip is more resistant to flow separation. The very bottom curve is the CFJ airfoil without the jet on. It has less stall AOA than the baseline airfoil because the injection and suction slot steps weaken the boundary layer and make the separation occur at a smaller AOA.

It needs to be pointed out that, when the AOA is more than 30 deg, the 0.1524 m chord airfoil creates a large blockage to the 0.3048 m × 0.3048 m wind tunnel. The airfoil suction surface experiences a more severe adverse pressure gradient than in the freestream conditions due to the forced diffusion caused by the wind-tunnel wall. The numerical simulation indicates that the CFJ airfoil in the freestream conditions has higher stall margin and maximum lift than in the wind tunnel [8]. In other words, the measured stall margin and maximum lift in the wind-tunnel tests are on the conservative side.

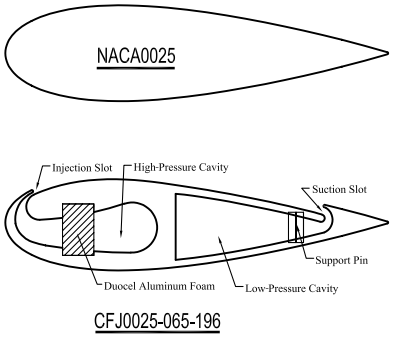

Fig. 1 Airfoil section of the baseline airfoil of NACA0025, CFJ airfoil CFJ0025-065-196, and CFJ airfoil CFJ0025-131-196.

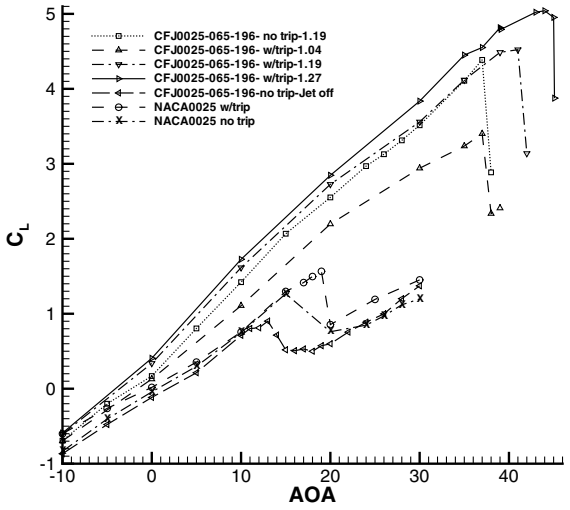

Fig. 2 Comparison of the measured lift coefficient for baseline NACA0025 and CFJ0025-065-196 airfoil.

Table 1 lists the aerodynamic parameters of the tripped baseline NACA0025 airfoil and the tripped CFJ0025-065-196 airfoil with injection total pressure coefficient of 1.27. Table 1 indicates that the $C_{L\max}$ of the CFJ0025-065-196 airfoil is 3.2 times that of the baseline airfoil, which is a 220% increase. The AOA stall margin is defined as the interval of the zero lift AOA to stall (maximum lift) AOA. The AOA stall margin of CFJ0025-065-196 airfoil is 2.53 times that of the baseline airfoil stall margin, an increase of 153%.

Figure 3 is the particle imaging velocimetry (PIV) measured velocity contours and streamlines of the attached flow of CFJ0025-065-196 airfoil at AOA of 43 deg, front part and rear part of the airfoil. The AOA of 43 deg is right before the stall AOA of 44 deg. They clearly show that the flow is very well attached at AOA of 43 deg with very high peak suction acceleration in the LE region. The flow merges to the mainflow in the TE region. The momentum coefficient at AOA of 43 deg is $C_\mu = 0.3$. The velocity contours in Fig. 3 also show the strong adverse pressure gradient of the main airfoil flow along the suction surface.

Because the PIV seeding is only done for the main flow, the PIV visualization shows little injection jet because the jet is not seeded. The detailed flow entraining or vortex structure in the mixing layer between the jet and main flow is not captured. In addition, the laser reflection on the aluminum airfoil surface also created a blur thin

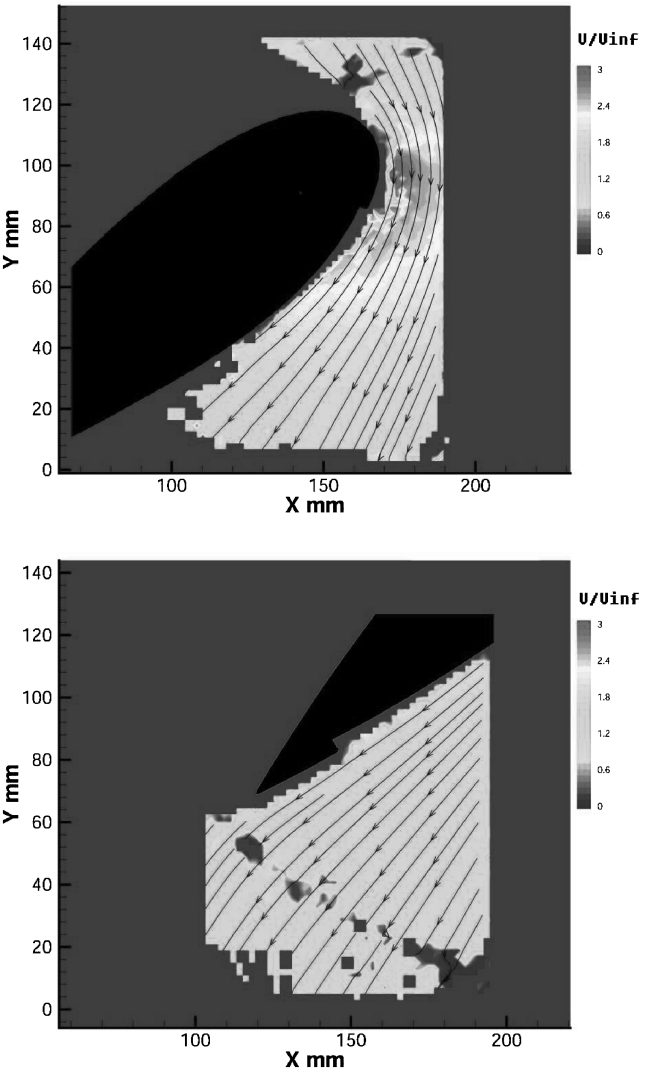

Fig. 3 PIV measured velocity contours and streamlines of the attached flow of CFJ0025-065-196 airfoil at AOA of 43 deg, top: front portion; bottom: rear portion.

layer on the airfoil surface, where no PIV data are acquired. The PIV images in this paper hence show primarily the qualitative feature of the flowfield such as attached or separated flow. The suction jet is able to be visualized to some extent because the mixing transports some seeding particles into the suction slot.

Figure 4 is the measured injection momentum coefficient of the CFJ0025-065-196 airfoil at three different injection total pressures. The momentum coefficient is defined as

$$C_\mu = \frac{\dot{m}_j V_j}{0.5\rho_\infty U_\infty^2 S} \tag{1}$$

The injection mass flow rate and velocity are determined by the injection total pressure and the main flow static pressure at the injection location. The injection total pressure is held constant while the AOA varies. When the AOA is increased, the LE suction is stronger and hence the local static pressure at the injection location decreases. The injection velocity therefore increases, and so do the

Table 1 Comparison of aerodynamic parameters between the tripped baseline airfoil and CFJ airfoil

Airfoil	$\text{AOA}_{C_L}=0$	$C_{\mu C_L}=0$	$\text{AOA}_{C_{L\max}}$	$C_{L\max}$	$C_{\mu C_{L\max}}$	$C_{D_{\min}}$ (AOA = 0 deg)
Baseline NACA0025	0 deg	0.0	19 deg	1.57	0.0	0.128
CFJ0025-065-196	−4 deg	0.187	44 deg	5.04	0.28	−0.036

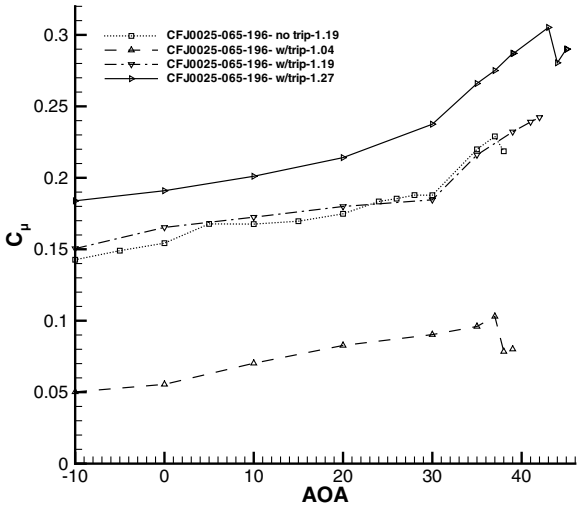

Fig. 4 Measured injection momentum coefficient for CFJ0025-065-196 airfoil.

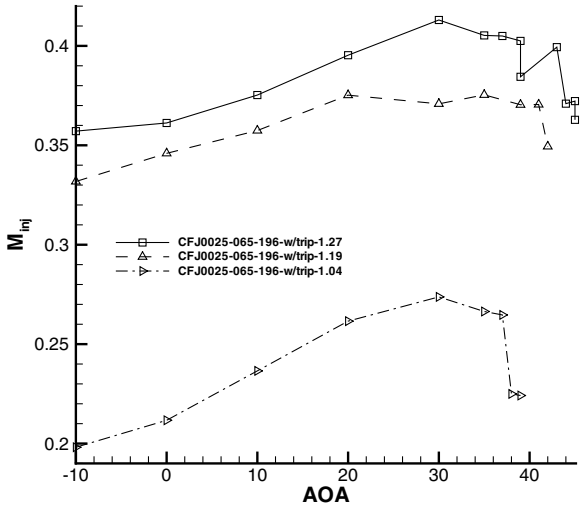

Fig. 6 Measured injection Mach number for CFJ0025-065-196 airfoil.

mass flow rate and the momentum coefficient as shown in Fig. 4. For the highest injection total pressure coefficient of 1.27, the momentum coefficient varies from 0.184 to 0.3. The lowest injection total pressure coefficient of 1.04 has the momentum coefficient varying from 0.05 to 0.1, which increases the $C_{L\max}$ by 113% and AOA stall margin by 100%. These results indicate that even the small momentum coefficient is very effective to enhance the lift and stall margin.

It needs to be pointed out that a jet kinetic energy coefficient is introduced in [3,4], which correlates the CFJ airfoil performance with different geometric parameters better than the momentum coefficient.

Figure 5 is the drag polar of the CFJ0025-065-196 airfoil. The drag coefficient of CFJ airfoil is significantly reduced and has a small region of negative drag (thrust). For example, at $C_L = 1$, for $C_\mu = 0.071$, the CFJ0025-065-196 airfoil drag reduction is 19%; for $C_\mu = 0.197$, the drag reduction is 90%, and this makes the L/D increased by 10 times. At lower C_L value with the total pressure coefficient of 1.27, the drag reduction is over 100% because the drag is negative and becomes thrust.

The airfoil drag can be decomposed into two parts: skin friction and pressure drag. As pointed out in [2], the skin friction drag of a CFJ airfoil does not vary much when the AOA changes. It is the large pressure resultant force in the streamwise direction that significantly decreases the total drag or generates thrust [2]. The low pressure at

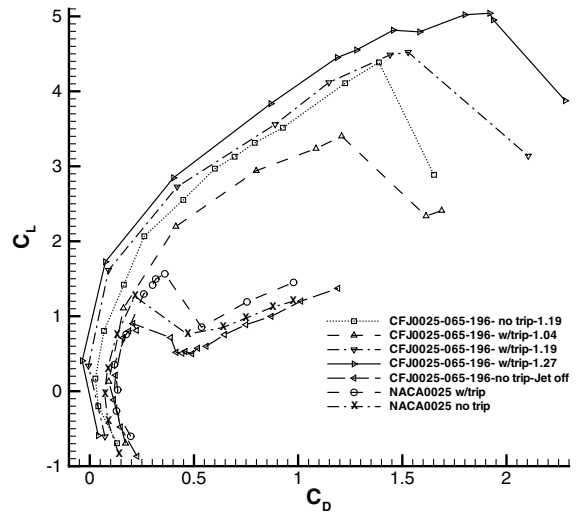

Fig. 5 Measured drag polar of CFJ0025-065-196 airfoil.

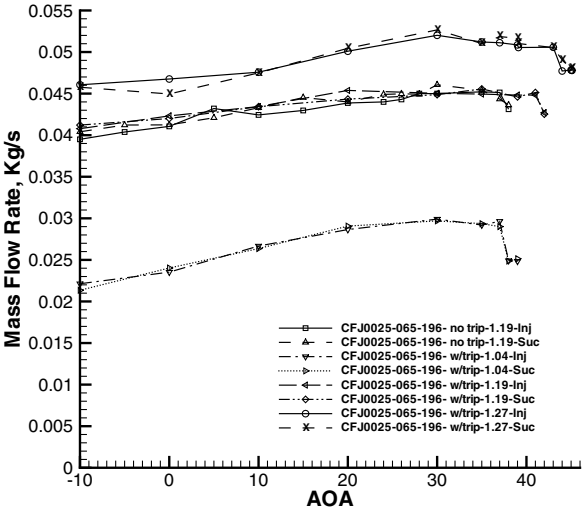

Fig. 7 Measured CFJ injection and suction mass flow rate of CFJ0025-096-196 airfoil.

LE due to the strong suction makes the primary contribution to the resultant pressure force pointing forward.

Figure 6 is the injection Mach number determined in the experiment by the procedure described in [3,4]. At AOA = 43 deg with the injection total pressure coefficient of 1.27, the injection Mach number is about 0.4. The velocity contours near the injection slot given in Fig. 3 show that the main flow velocity is about 3 times of the incoming freestream velocity. The freestream Mach number is 0.1. Hence the Mach number of the main flow near the injection slot is about 0.3. The dissimilarity of the velocity may enhance the shear layer mixing. Because the jet was not seeded for PIV visualization, it is not clear if there exists a large vortex structure caused by the velocity dissimilarity [9].

Figure 7 plots the mass flow rate of the injection and suction vs AOA at different injection total pressures. The CFJ airfoil requires that the injection mass flow rate be equal to the suction mass flow rate to achieve the zero-net mass-flux flow control. Figure 7 indicates that they indeed agree very well with the maximum difference of 3.9%.

B. Jet Instability

In the experiment, it is observed that there is a limit of the jet mass flow rate to maintain the stability of the flow. Below the limit, increasing the jet mass flow (momentum coefficient) will make the flow attached and increase the lift and stall margin. However, if the jet mass flow rate exceeds the limit, the whole flowfield breaks down

and a large separation occurs. The turbulent shear layer due to jet mixing is complicated and could be dominant by the coherent structure [10]. The reason of the flowfield breakdown is not clear at this time and may be speculated as the following two aspects:

1) The mixing shear layer loses stability due to the large difference of the Mach number, or the so-called convective Mach number,

$$M_c = \frac{U_1 - U_2}{a_1 + a_2} \tag{2}$$

where U_1, U_2, a_1, and a_2 are the velocity and speed of sound of the main flow and the jet. The density and velocity ratio between the main flow and jet also have an effect on the mixing shear layer stability [10,11].

2) The high momentum of the injection jet creates a large centrifugal force, which makes the jet detached and the flowfield collapse.

Because of the time limitation of this research, the details of the jet instability phenomenon were not studied. More detailed research of the jet stability limit from both computational fluid dynamics (CFD) and experiment will be conducted in the future.

IV. Conclusions

This research has demonstrated the high performance of the coflow jet airfoil concept in wind-tunnel tests. The CFJ airfoils are shown to drastically increase lift, stall margin, and drag reduction. With the momentum coefficient varying from 0.1 to 0.30, the maximum lift of the smaller size CFJ airfoil is increased by 113 to 220%, and the angle of attack operating range (stall margin) is increased by 100 and 153%. The minimum drag coefficient is reduced by 30 to 127% with the momentum coefficient varying from 0.055 to 0.192. A negative drag (thrust) is produced when the momentum coefficient is high.

In the experiment, it is observed that there is a limit of the jet mass flow rate in maintaining the stability of the flow. Below the limit, increasing the jet mass flow (momentum coefficient) will make the flow attached and increase the lift and stall AOA. However, if the jet mass flow rate exceeds the limit, the whole flowfield breaks down and a large separation occurs. It is speculated that the instability may be attributed to the large dissimilarity of the jet and the main flow, and the large centrifugal force of the jet when the jet velocity is high. The exact mechanism is not clear yet and will be studied in future research.

Acknowledgments

We would like to thank the NASA Langley Research Center (LaRC) for supporting this research under the contract NNL04AA39C of NRA-03-LaRC-02. We would also like to thank R. Gaeta at Georgia Tech Research Institute for his advice to use Duocel aluminum foam to achieve uniform injection flow.

References

[1] Zha, G.-C., Gao, W., and Paxton, C., "Jet Effects on Co-Flow Jet Airfoil Performance," *AIAA Journal* (to be published); also AIAA Paper 2006-0102, 2007.

[2] Zha, G.-C., and Paxton, D. C., "A Novel Flow Control Method for Airfoil Performance Enhancement Using Co-Flow Jet," *Applications of Circulation Control Technologies*, edited by R. D. Joslin, and G. S. Jones, Vol. 214, Progress in Astronautics and Aeronautics, AIAA, Reston, VA, 2006, pp. 293–314, Chap. 10.

[3] Zha, G.-C., Carroll, B., Paxton, C., Conley, A., and Wells, A., "High Performance Airfoil with Co-Flow Jet Flow Control," AIAA Paper 2005-1260.

[4] Zha, G.-C., Paxton, C., Conley, A., Wells, A., and Carroll, B., "Effect of Injection Slot Size on High Performance Co-Flow Jet Airfoil," *Journal of Aircraft*, Vol. 43, No. 4, 2006, pp. 987–995.

[5] Zha, G.-C., "High Performance Airfoil with Co-Flow Jet Flow Control," NASA Final Report to LaRC Contract NNL04AA39C, Aug. 2004.

[6] Aguirre, J., and Zha, G.-C., "Design and Study of "Engineless" Airplane Using Co-Flow Jet Airfoil," AIAA Paper 2007-4441, June 2007.

[7] Greitzer, E. M., Tan, C. S., and Graf, M. B., *Internal Flow*, Cambridge Univ. Press, Cambridge, U.K., 2004.

[8] Zha, G.-C., Gao, G., and Paxton, C. D., "Numerical Simulation of Airfoil Flows Using Co-Flow Jet Flow Control," AIAA Paper 2006-1060, 2006.

[9] Papamoschou, D., and Roshko, A., "The Compressible Turbulence Shear Layer: An Experimental Study," *Journal of Fluid Mechanics*, Vol. 197, 1988, pp. 453–477.

[10] Brown, G., and Roshko, A., "On Density Effects and Large Scale Structure in Turbulent Mixing Layers," *Journal of Fluid Mechanics*, Vol. 64, 1974, pp. 675–816.

[11] Strykowski, P., Krothapalli, A., and Jendoubi, S., "The Effect of Counterflow on the Development of Compressible Shear Layers," *Journal of Fluid Mechanics*, Vol. 308, 1996, pp. 63–69.

J. Gore
Associate Editor